Donor/Acceptor Coupling in Mixed-Valent Dinuclear Iron Polypyridyl Complexes: Experimental and Theoretical Considerations

C. Michael Elliott,*,† Daniel L. Derr,† Suzanne Ferrere,†,‡ Marshall D. Newton,*,§ and Y.-P. Liu§

Contribution from the Department of Chemistry, Colorado State University, Ft. Collins, Colorado 80523-1872, and Chemistry Department, Brookhaven National Laboratory, Upton, New York 11973

Received December 28, 1995[⊗]

Abstract: Coupling between donor and acceptor orbitals for optically-induced intervalence electron transfer processes has been considered for a series of rigid mixed-valent dinuclear tris(2,2′-bipyridine)iron complexes. Each of the four complexes considered contains three saturated bridges which link the two tris(2,2′-bipyridine)iron moieties. The bridging linkages are $-CH_2CH_2-$, $-CH_2CH_2CH_2-$, $-CH_2OCH_2-$, and $-CH_2SCH_2-$. Despite differences in the composition of the bridges X-ray diffraction and/or molecular dynamics calculations show that the metal−metal separation and relative bipyridine orientations among all four complexes are nearly identical. Consequently, the only factor which differs significantly among these complexes and which might affect the donor−acceptor coupling in the mixed-valent forms is their connectivity. These complexes thus provide a unique opportunity to focus on potential superexchange coupling in the absence of ambiguities introduced by other structural and energetic considerations. Theories developed by Mulliken and Hush have been applied to intervalence charge-transfer transitions in order to obtain values of the coupling matrix elements, H_{12}. Configuration interaction calculations were also carried out for each of the $[Fe_2(L)_3]^{5+}$ complexes to provide theoretical values of H_{12} and the effective donor/acceptor separation distances (r_{DA}). Experimental and theoretical results for H_{12} are in excellent agreement and indicate that the bridging moieties are either unimportant in the donor/acceptor coupling or, in one case, actually reduce the coupling compared to the "bridge-free" system. The calculated r_{DA} values are within 0.01 Å of the Fe−Fe distances.

Introduction

Intramolecular electron-transfer reactions are of considerable practical and theoretical interest. For example, essential biological processes such as bacterial photosynthesis[1,2] and respiration[3,4] involve electron transfers between redox centers rigidly positioned within protein structures. In some instances respective redox partners are located within only a few angstroms of one another, and in others they are separated by substantial distances. Thus, developing a better understanding of the mechanisms of electronic coupling in rigidly linked donor/acceptor assemblies is an important goal. Of particular relevance are questions about how the connective framework participates in coupling the donor and acceptor orbitals. When donor and acceptor sites are separated by large distances it is well established that direct or "through-space" coupling is too weak to account for experimentally observed rates of electron transfer. In these instances the rates can be rationalized only by considering coupling through the σ and/or π bonding framework connecting the two centers (superexchange). At shorter distances, however, the situation becomes less clear.

Designing chemical systems which can be used to experimentally address the importance of intramolecular superexchange coupling between a donor and an acceptor is an intrinsically difficult proposition. The donor/acceptor separation, their relative orbital orientations, the relative and absolute orbital energies, and the connectivity can all influence donor/acceptor coupling.[5] Few chemical systems allow for well-defined changes in donor/acceptor connectivity without simultaneous changes in one or more of the other variables which could alter the coupling. In the present study a group of four symmetrical triply-bridged dinuclear iron complexes are considered. Energy-minimized structures obtained from molecular dynamics calculations are shown in Figure 1, and the ligand structures are given below. These complexes possess several

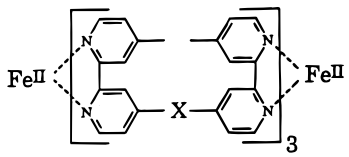

3

I. X = $(CH_2)_2$
II. X = $(CH_2)_3$
III. X = CH_2-O-CH_2
IV. X = CH_2-S-CH_2

features which make them uniquely suited for studies of bridge-

† Colorado State University.
‡ Present address: National Renewable Energy Laboratory, Golden, CO 80401.
§ Brookhaven National Laboratory.
⊗ Abstract published in *Advance ACS Abstracts,* May 1, 1996.

(1) Deisenhofer, J.; Michel, H. In *Chlorophylls*; Scheer, H., Ed.; CRC: Boca Raton, FL, 1991; p 613.
(2) El-Kabbani, O.; Chang, C. H.; Tiede, D.; Norris, J.; Schiffer, M. *Biochemistry* **1991**, *30*, 5361.
(3) Iwata, S.; Ostermeier, C.; Ludwig, B.; Michel, H. *Nature* **1995**, *376*, 660.
(4) Tsukihara, T.; Aoyama, H.; Yamashita, E.; Tomizaki, T.; Yamaguchi, H.; Shinzawa-Itoh, K.; Nakashima, R.; Yaono, R.; Yoshikawa, S. *Science* **1995**, *269*, 1069.
(5) Sutin, N. *Progr. Inorg. Chem.* **1983**, *30*, 441.

S0002-7863(95)04297-1 CCC: $12.00

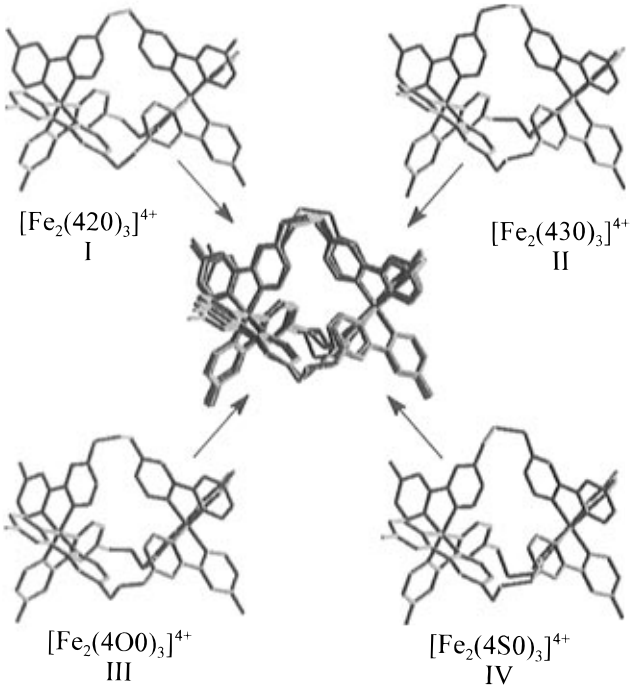

Figure 1. Structures of **I**−**IV** obtained from molecular mechanics calculations. The central portion of the figure shows the superposition of the four individual structures.

mediated superexchange. First, despite significant differences in the structures of the moieties bridging the bipyridines the metal−metal separation is virtually the same for all four molecules (ca. 7.61 ± 0.03 Å). Figure 1 shows the individual structures of **I**−**IV** obtained from molecular mechanics calculations. In the central part of the figure the four individual structures are overlaid. As is clear from this structural presentation the only major difference among the four complexes lies in the bridges.

The visible spectrum of each complex is essentially indistinguishable from that of $[Fe(DMB)_3]^{2+}$ (DMB = 4,4′-dimethyl-2,2′-bipyridine), consistent with there being a weak orbital interaction between the two metal complex chromophores in the ground state. Detailed electrochemical studies have been conducted on **I**−**IV**, and the results for **I** and **II** are reported in ref 6. To summarize the pertinent aspects of these results, because of the close proximity of the two positively charged metal centers there is a significant electrostatic influence on the redox potentials of each of the two the metal sites relative to one another and relative to the monomeric complex $[Fe(DMB)_3]^{2+}$. For example, the first metal-centered oxidation for the dinuclear complexes (3+/2+) is shifted by ca. 90 mV to more positive potentials relative to the 3+/2+ couple of $[Fe(DMB)_3]^{2+}$. Additionally, the second of the two metal-centered 3+/2+ oxidations is shifted positively of the first by ca. 70 mV. As a consequence, the $[Fe_2(L)_3]^{5+}$ mixed valence form of each of these complexes has considerable thermodynamic stability with respect to disproportionation and, thus, will exist in significant relative concentration in solution.

The $[Fe_2(L)_3]^{5+}$ mixed-valence form of each dinuclear complex exhibits a weak, but experimentally measurable, intervalence charge transfer (IT) transition in the near-infrared. By application of theories developed by Mulliken[7] and Hush[8] to these data experimental values of the coupling matrix element, H_{12}, may be obtained. Configuration interaction calculations have also been carried out for each of the $[Fe_2(L)_3]^{5+}$ complexes from which theoretical values of H_{12} are obtained. Below we consider the results from these experimental and theoretical treatments. The near-isostructural nature of the four complexes allows the discussion to focus on how the different bridging linkages affect the donor/acceptor coupling in the absence of ambiguities introduced by other structural and energetic considerations which might influence H_{12}.

Experimental Section

Materials, Instrumentation, Complex Preparation, and Analysis. The preparations of 1,2-bis[4-(4′-methyl-2,2′-bipyridyl)]ethane (420)[9] and 1,3-bis[4-(4′-methyl-2,2′-bipyridyl)]propane (430)[6] have been reported previously. The preparations of bis[4-(4′-methyl-2,2′-bipyridyl)]methyl]ether (4O0), bis[[4-(4′-methyl-2,2′-bipyridyl)]methyl] sulfide (4S0), complexes **I-IV**, along with their characterizations (^{1}H-NMR, ES-MS and elemental analysis) are included as supporting information. Also included as supporting information are descriptions of materials and instrumentation.[10,11]

Electrochemistry. Cyclic voltammetry (CV) was performed on a 0.5 mM solution of each $[Fe_2(L)_3](PF_6)_4$ complex. Data was collected using a BioAnalytical Systems BAS 100 Electrochemical Analyzer and a standard three-electrode cell with 0.1 M $TBAPF_6$ in ACN as electrolyte. The experimental CV data for each complex was fit using Digisim (Bioanalytical Systems) in order to determine $E_{1/2}$'s for the two closely spaced waves: 6+/5+ and 5+/4+. The algorithm Digisim utilizes to simulate electrochemical data, developed by Rudolph, is reported elsewhere.[12] The following model parameters were used: β (the exponential grid factor) = 0.5; potential step between calculations = 0.005 V; Gauss−Newton iterations = 1; noise level = 0.0; D^*/k^* (a ratio of diffusion coefficient to reaction layer) = 50; $X_{max}/(D_t)^{1/2}$ (maximum distance for diffusion) = 6. The fit was conducted assuming a planar electrode (no edge effects) with semiinfinite diffusion. The following fit parameters were set at their experimental values: $E_{initial}$ (+0.5 V); $E_{reverse}$ (+1.5 V); E_{final} (+0.5 V); scan rate (0.01 V/s); temperature (298 K); number of cycles (1); electrode area (0.07 cm^2); analyte concentration (0.5 mM). Heterogeneous and homogeneous rate constants for all electron transfer reactions were effectively infinite (1×10^{10}), and α, the transfer coefficient, for both half reactions was held at 0.5. Parameters that were allowed to vary during the fit were $E_{1/2}^{6+/5+}$, $E_{1/2}^{5+/4+}$, and D, the diffusion coefficient, for each species, 6+, 5+, and 4+. The comproportionation constant, K_{com}, was determined from the calculated CV best fit to the experimental data.

Molecular Mechanics and Dynamics Calculations. The Dreiding force field[13a] was modified slightly, as follows, for this work. All nonbonded interactions were considered in energy calculations (i.e., the nonbond cutoff distance was effectively infinite). A distance-independent dielectric constant (ϵ) of unity was employed. The nonbond parameters (R_0 and D_0) describing the interaction between two dissimilar atoms were taken as the arithmetic mean of the parameters for the two atom types.

Charge distributions were calculated using the *QEq* charge equilibration scheme,[13b] which is an iterative process. It was assumed complete when the charge on each hydrogen atom varied less than 0.0005 of an electron in succeeding steps.

Molecular modeling calculations on the four $[Fe_2(L)_3](CF_3SO_3)_4$ complexes were carried out using Biograf, Versions 2.2 and 3.21

(6) Ferrere, S.; Elliott, C. M. *Inorg. Chem.* **1995**, *34*, 5818.
(7) Mulliken, R. S. *J. Am. Chem. Soc.* **1950**, *72*, 600. Mulliken, R. S. *J. Am. Chem. Soc.* **1952**, *74*, 811. Mulliken, R. S. *J. Phys. Chem.* **1952**, *56*, 801.
(8) Hush, N. S. *Prog. Inorg. Chem.* **1967**, *8*, 391.
(9) Serr, B. R.; Andersen, K. A.; Elliott, C. M.; Anderson, O. P. *Inorg. Chem.* **1988**, *27*, 4499.
(10) Sawyer, D. T.; Roberts, J. L. *Experimental Electrochemistry for Chemists*; Wiley: New York, 1974.
(11) Gould, S.; Strouse, G. F.; Meyer, T. J.; Sullivan, P. B. *Inorg. Chem.* **1991**, *30*, 2942.
(12) (a) Rudolph, M. *J. Electroanal. Chem.* **1991**, *314*, 13. (b) Rudolph, M. *J. Electroanal. Chem.* **1992**, *338*, 85. (c) Rudolph, M. In *Physical Chemistry: Principles, Methods and Applications*; Rubenstein, I., Ed.; Marcel Dekker: New York, 1995; pp 81−129.
(13) (a) Mayo, S. L.; Olafson, B. D.; Goddard, W. A., III. *J. Phys. Chem.* **1990**, *94*, 8897. (b) Rappé, A. K.; Goddard, W. A. *J. Phys. Chem.* **1991**, *95*, 3358. (c) Stouch, T. R.; Jurs, P. C. *J. Chem. Int. Comput. Sci.* **1986**, *26*, 4.

Table 1. Calculated Distance Values (Å)

L	r_{M-M} values for $[Fe_2(L)_3]^{4+}$ from molecular mechanics calcns	r_{DA} values for $[Fe_2(L)_3]^{5+}$ from GMH[a] result (eq 6)	
		full complex	bridges removed
420	7.64	7.63	7.62
430	7.63	7.62	7.64
4O0	7.61	7.61	7.62
4S0	7.59	7.58	7.60

[a] Generalized Mulliken Hush.[25]

(Molecular Simulations, Burlington, MA). Initial structures for the complexes were built to resemble the published $[Fe_2(420)_3](SO_3CF_3)_4$ crystal structure.[9] The cation portion of the complexes, $[Fe_2(L)_3]^{4+}$, minimized to conformers which qualitatively resembled the cation portion of the crystal structure. Anions were then constrained to the positions found in the crystal structure. With the anions constrained, the local minimum was found as described below. Simulated annealing was used as the method of conformational searching. Each initial structure was heated from 0 to 600 K and cooled back to 0 K with a symmetrical temperature ramp of 10° every 10 fs. The time step between structure calculations was 1 fs. Twenty annealing cycles were used, and the local minimum for each 0 K structure was found by the procedure outlined below. The three resulting structures with the lowest energy were used to calculate the distances in Table 1.

To find the local energy minimum for any high energy structure, a charge equilibration with zero total charge was followed by an energy minimization (stopped when the root mean square (rms) residual force constant was less than 0.001 (kcal/mol)/Å), and then another charge equilibration, etc. until no change occurred in the minimization step.

Molecular volumes were calculated by the uniform finite element method.[13c] van der Waals radii were scaled by 0.890, and in the solvent-excluded volumes a probe radius of 1.4 Å was used. Grid calculations had a dot density of 4 $Å^{-1}$.

Titrations. Titrations were done on 0.015−0.02 M solutions of $[Fe_2(L)_3](PF_6)_4$ in ACN. Each solution was treated with small solid aliquots of $NOBF_4$ to oxidize the complex from the 4+ through the 5+ to the 6+ oxidation state. The amount of $NOBF_4$ in each addition (approximately 0.1 molar equiv) was not premeasured. Each addition was followed by a few seconds of mixing, and then a spectrum of the solution was acquired from 2500 to 600 nm. A very low intensity band in the near IR first grew in and then disappeared in the course of the titration for each complex. The color of each solution changed from red to green, as well. The titration was assumed complete when there was no change in the spectrum upon further addition of oxidizing agent. Oxidized solutions of $[Fe_2(L)_3]$ were stable for at least several hours.

Results

X-Ray Crystallographic and Molecular Mechanics Results. The X-ray structural details for $[Fe_2(420)_3](SO_3CF_3)_4$ have been reported previously.[9] A preliminary X-ray study of $[Fe_2(430)_3](SO_3CF_3)_4$ has also been reported, although the structural details were not included because of severe disorder in the anions.[6] Attempts to model the disordered anions were completely unsuccessful. However, the cationic portion of the molecule was successfully modeled, even down to the level of a 50/50 disorder in the central methylene carbon of each alkyl bridge. Despite numerous attempts, diffraction quality crystals of $[Fe_2(4S0)_3]^{4+}$ and $[Fe_2(4O0)_3]^{4+}$ have not yet been obtained.

Comparisons between X-ray structures and the structures obtained from the molecular mechanics calculations for $[Fe_2(420)_3]^{4+}$ and $[Fe_2(430)_3]^{4+}$ are instructive. When the X-ray and modeled structure of $[Fe_2(420)_3]^{4+}$ are overlayed the two are effectively identical (i.e., the relative position of each atom in the two structures agrees to within 0.16 Å). Likewise, except for the disordered alkyl bridge, the modeled and X-ray structures for $[Fe_2(430)_3]^{4+}$ superimpose, as well. This excellent agreement between the X-ray and modeled structures provides for a high level of confidence that the modeled structures are meaningful representations of these complexes both in the solid state and in solution. Since the modeling calculations represent gas phase results, the structures of the dinuclear cationic units appear essentially unaffected by crystal packing forces—otherwise differences would be evident between the two methods of determining the structures.

Since diffraction quality crystals of $[Fe_2(4S0)_3]^{4+}$ and $[Fe_2(4O0)_3]^{4+}$ have not been obtained, modeling must be used to make any structural comparisons with $[Fe_2(420)_3]^{4+}$ and $[Fe_2(430)_3]^{4+}$. As shown in Figure 1 all four structures are very nearly superimposable if the bridges are ignored. The Fe−Fe separations are the same to within ± 0.03 Å (Table 1, column 1), and the relative orientations of the bipyridines are all very similar (see Figure 1). The only significant structural differences, again, lie in the composition and orientations of the respective bridges.

Electrochemical Determination of K_{com}. The degree of comproportionation between the fully oxidized ($[Fe_2(L)_3]^{6+}$) and fully reduced ($[Fe_2(L)_3]^{4+}$) dinuclear complexes (to produce the mixed valent form ($[Fe_2(L)_3]^{5+}$)) can be established from experimentally determined voltammetric potentials for the 5+/4+ and 6+/5+ redox processes. It is important to acquire values for the comproportionation constant, K_{com}, because for these weakly interacting systems (i.e., small K_{com}) there is always a significant amount of disproportionation of the $[Fe_2(L)_3]^{5+}$ mixed-valence species. Consequently, any effort to quantitate the concentration of mixed-valence species in solution must take into account disproportionation.

The value of K_{com} is straightforwardly extracted from ΔE, the difference in $E_{1/2}$ between the 5+/4+ and 6+/5+ redox processes. For weakly interacting systems, however, ΔE is relatively small (e.g., ca. 70 mV in the present cases); thus, the individual voltammetric waves for the respective processes are not well resolved. The values for $E_{1/2}(5+/4+)$ and $E_{1/2}(6+/5+)$ must, therefore, be obtained by fitting the experimental data to a mathematical model.

Detailed electrochemical studies of $[Fe_2(420)_3]^{n+}$ and $[Fe_2(430)_3]^{n+}$ have previously been reported along with calculated values for K_{com}.[6,9] In these studies the individual $E_{1/2}$ values were obtained by fitting Osteryoung square wave voltammetry (OSWV) data to an ideal reversible EE mechanism.[14] $[Fe_2(4S0)_3]^{n+}$ and $[Fe_2(4O0)_3]^{n+}$ were not considered as part of this earlier study. Alternatively, values of K_{com} for all four dinuclear complexes under consideration here were obtained from cyclic voltammetry measurements. A reversible EE mechanism was fit to digitized voltammograms with Digisim (BioAnalytical Systems), and values of $E_{1/2}(4+/5+)$, $E_{1/2}(5+/6+)$, and K_{com} were calculated directly from the fit. Table 2 lists the values of K_{com} reported in ref 6 and 9 along with those resulting from fits of the CV data. The good agreement between the values obtained using the two different electrochemical techniques and different fitting methods for $[Fe_2(420)_3]^{n+}$ and $[Fe_2(430)_3]^{n+}$ validates both approaches. The absolute values of K_{com} are such that when solutions of $[Fe_2(L)_3]^{4+}$ are oxidized by exactly 1 equiv the resulting solution will be approximately 70% mixed valent, $[Fe_2(L)_3]^{5+}$, and 15% each of $[Fe_2(L)_3]^{4+}$ and $[Fe_2(L)_3]^{6+}$.

Intervalence Charge Transfer Transition of Mixed Valence $[Fe_2(L)_3]^{5+}$. The $[Fe_2(L)_3]^{5+}$ mixed valence form of each dinuclear complex exhibits a weak intervalence charge transfer (IT) transition in the near IR. Due to the low intensity and energy of the transition, concentrated solutions (0.015−0.020

(14) O'Dea, J. J.; Osteryoung, J.; Osteryoung, R. A. *Anal. Chem.* **1981**, *53*, 695.

Table 2. Electrochemical Data for $[Fe_2(L)_3]^{n+}$ [a]

L	$E^{6+/5+}$(V)	$E^{5+/4+}$(V)	ΔE(V)	K_{com}(CV)	K_{com}(OSWV)[b]
420	1.081 ± 0.010	1.012 ± 0.010	0.069 ± 0.010	15 ± 5	15.9
430	1.048 ± 0.010	0.973 ± 0.010	0.070 ± 0.010	18 ± 6	17.1
4O0	1.104 ± 0.010	1.036 ± 0.010	0.068 ± 0.010	14 ± 5	
4S0	1.086 ± 0.010	1.021 ± 0.010	0.065 ± 0.010	12 ± 4	

[a] Potentials are reported vs SSCE. [b] From ref 6.

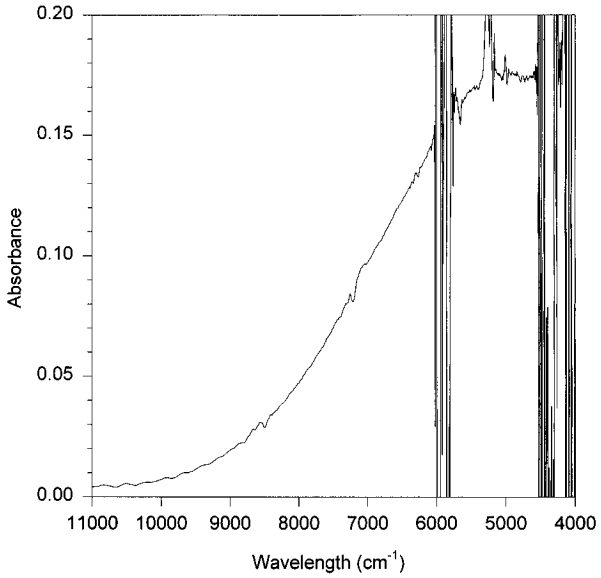

Figure 2. Corrected (see text) near-IR spectrum obtained during the titration of $[Fe_2(430)_3](PF_6)_4$ with $NOBF_4$(s) in ACN at 25 °C. This spectrum corresponds to the point in the titration with the highest absorbance at 5000 cm^{-1}.

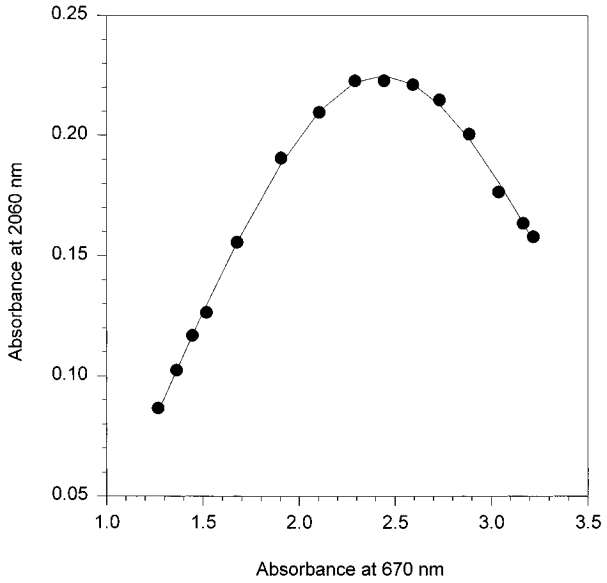

Figure 3. Plot of absorbance at the IT band maximum vs absorbance at 670 nm for the titration of 0.02 M $[Fe_2(4O0)_3](PF_6)_4$ in ACN with $NOBF_4$(s) at 25 °C. The absorbance values are uncorrected. The solid circles are the experimental data; the solid line is the best fit to the theoretical relation described in the text.

M) and moderately long path length cells (1 cm) were required in these spectral titrations. Even so, the spectrum for each complex is complicated by solvent overtone vibrational bands and by the fact that the individual oxidized and reduced FeL_3 halves of each complex have small but significant absorbances within the wavelength region where the IT transition occurs. Figure 2 is a corrected spectrum of the IT transition for $[Fe_2(430)_3]^{5+}$. It was obtained by subtracting the spectrum of $[Fe_2(430)_3]^{4+}$ (obtained from the initial solution before adding any oxidant) multiplied by one half and the spectrum of $[Fe_2(430)_3]^{6+}$ (obtained at the end of the titration) multiplied by one half from the spectrum at the midpoint of the titration (*vide infra*). Any residual absorbance from individual $Fe(L)_3^{3+}$ and $Fe(L)_3^{2+}$ chromophores should be removed by this manipulation, leaving only the IT transition. The IT band for each of the other mixed valence dinuclear complexes is similar.

Molar extinction coefficients for the IT transition, ϵ_{IT}, were obtained from spectral redox titrations. The progress of the titration was followed by comparing the change in absorbance at the wavelength maximum of the IT transition, λ_{IT}, with the absorbance change at a monitoring wavelength, λ_{mon} (either 670 or 700 nm). At λ_{mon}, the 6+ oxidation state has a larger extinction coefficient than does the 5+, both of which are greater than the extinction coefficient of the 4+ complex. It should be noted that the extinction coefficient of the 5+ species at λ_{mon} is not exactly the arithmetic mean of the extinction coefficients of the 4+ and 6+ species; therefore, it must be treated as an independent variable in any fit (*vide infra*).

Figure 3 shows the results of a typical titration. The points are the experimental data, and the solid line is the theoretical fit. The relationship used for the fit was derived by combining the mass balance relationship, Beer's Law (at λ_{mon} and λ_{IT}), and the comproportionation equilibrium expression. It contains seven variables: K_{com}, the three ϵ's at λ_{mon} (for the 4+, 5+, and 6+ oxidation states), and the three ϵ's at λ_{IT}. The value of K_{com} for each fit was constrained to be the one obtained from the electrochemical measurement. The ϵ values at λ_{mon} for the 4+ and 6+ oxidation states were obtained from the initial and final spectra, respectively. The ϵ value at λ_{mon} for the mixed valence 5+ state and all three ϵ values at λ_{IT} were obtained from the fits.[15] The quality of the fit shown in Figure 3 is typical for all four of the compounds under consideration. The values of ϵ_{IT} obtained from these titration are given in Table 3.

Table 3. Spectral Data for the IT Band of $[Fe_2(L)_3]^{5+}$

L	ν_{IT} (cm^{-1})	$\Delta\nu_{1/2}$ (cm^{-1}) (meas)[a]	$\Delta\nu_{1/2}$(cm^{-1}) (calc)[b]	ϵ (cm^{-1} M^{-1})
420	7000 ± 400	4000 ± 400	4000	1.8 ± 0.2
430	5000 ± 400	4400 ± 800	3400	19 ± 1
4O0	5500 ± 600	4600 ± 600	3600	10 ± 1
4S0	5600 ± 600	4000 ± 800	3600	8 ± 1

[a] See discussion in text. [b] Values were calculated from eq 1.

Experimental Determination of the Resonance Integral, H_{12}. By employing well-known theories developed by Mulliken and Hush (MH), the resonance integral, H_{12}, for the donor/acceptor orbital interaction for weakly coupled mixed valence species can be calculated from measurable spectral and structural parameters.[7,8]

In the high temperature limit the IT spectrum should approach being Gaussian in shape.[8] Furthermore, the band width at half maximum, $\Delta\nu_{1/2}$, should relate to the frequency maximum of

(15) The values of ϵ at λ_{IT} for the 4+ and 6+ oxidation states could have been constrained to be the values obtained from the initial and final spectra. However, given the signal-to-noise ratio in this spectral region and the likely measurement error, it seemed more reasonable to obtain these values from the fit since it is significantly overdetermined.

Table 4. Values of H_{12} (cm^{-1}) for $[Fe_2(L)_3]^{5+}$

		theoretical[b]	
L	expt[a]	full complex	bridges removed
420	19 ± 3	46	97
430	57 ± 9	52	52
4O0	44 ± 8	55	60
4S0	37 ± 8	49	48

[a] Equation 2, using spectral data. [b] Equation 5, using adiabatic quantities from INDO/S CI calculations.

the IT absorption, ν_{IT}, as follows:

$$\Delta\nu_{1/2} = \sqrt{2310\nu_{IT}} \tag{1}$$

Due to interference from solvent vibrational overtones on the low energy side of the IT bands experimental $\Delta\nu_{1/2}$ values were obtained by assuming the bands to be Gaussian and taking the difference between ν_{max} and ν at half the maximum absorbance on the high energy side of the band and doubling that value. The spectral values so determined and those calculated from eq 1 are presented in Table 3. There is generally good agreement between the calculated and experimental numbers.

Again, following the approach of Hush and Mulliken,[7,8] H_{12} (cm^{-1}) can be calculated using the relation

$$H_{12} = (0.0206/r)\sqrt{\epsilon(\Delta\nu_{12})\nu_{IT}} \tag{2}$$

where $\Delta\nu_{1/2}$, ν_{IT}, and ϵ_{IT} have their previously defined meanings and r is the separation between the donor and acceptor sites. The second column of Table 4 lists values of H_{12} calculated using eq 2 for the IT transitions of each of the four dinuclear complexes. In these calculations the experimentally measured values of $\Delta\nu_{1/2}$ were employed. The value of r was taken as the Fe−Fe internuclear separation obtained from the molecular mechanics calculation listed in Table 1, column 2.

Discussion

Intervalence Charge Transfer Spectra. The energy of an IT transition is equal to the total reorganizational energy for symmetrical mixed valence species[8,16]

$$E_{op} = E_{out} + E_{in} + \lambda_{SO} \tag{3}$$

where E_{op} is the energy of the transition, E_{out} and E_{in} are the outer-sphere and inner-sphere reorganizational energies, respectively, and λ_{SO} is the spin−orbit coupling correction (ca. 460 cm^{-1} for Fe).[16] The 3+/2+ self-exchange reaction for mononuclear $Fe(phen)_3$ has an inner sphere reorganizational energy which is essentially zero.[17] Therefore, it can be assumed that the IT band energies listed in Table 3 for the $[Fe_2(L)_3]^{5+}$ complexes directly reflect $E_{out} + \lambda_{SO}$. The very weak coupling in these systems argues that they are valence localized. Comparisons of these ν_{IT} values with similar data obtained from a large variety of other mixed valence metal complexes suggest, on first consideration, that ν_{IT} (and, thus E_{out}) for $[Fe_2(L)_3]^{5+}$ is rather small.[18] Typically, ν_{IT} values as low as these are associated with complexes which have delocalized valence or which undergo rapid thermal intervalence electron transfer on the time-scale of solvent dynamics. Such explanations for the small magnitude of ν_{IT} values listed in Table 3 are not reasonable based on values of H_{12} given in Table 4. Several models have been employed which estimate the E_{out} for dinuclear mixed valence metal complexes.[16a,19,20] The details of various approaches differ, but each considers a pair of spherical or elliptical metal complex centers (the donor and acceptor) located in a dielectric continuum. In the simplest case[16a] where the donor and acceptor are treated as two spheres the relation takes the form

$$E_{out} = (\Delta q)^2\left(\frac{1}{2a_1} + \frac{1}{2a_2} - \frac{1}{r}\right)\left(\frac{1}{D_{op}} - \frac{1}{D_s}\right) \tag{4}$$

where Δq is the number of electrons transferred, a_1 and a_2 are the respective radii of the donor and acceptor, r is the distance between the centers of the donor and acceptor, and D_{op} and D_s are the optical and static dielectric constants of the solvent. The more complex models also contain the solvent dielectric term $[1/D_{op} - 1/D_s]$. The differences in the various approaches primarily lie in the geometric factors used for the donor and acceptor.

Equation 4 is strictly applicable only to cases where $a_1 + a_2 \leq r$; however, it has been applied to cases where $a_1 + a_2 > r$ with considerable success.[16a] Generally, E_{out} obtained from any of these models tends to overestimate the experimental outer-sphere reorganizational energy. Moreover, E_{out} calculated assuming elliptical cavities which encompass both a_1 and a_2 (so-called "minimum enclosing volume condition")[16a] are generally slightly smaller than values obtained by the simpler two-sphere model.

In order to apply eq 4 (or any of its more sophisticated analogs), an estimation of the apparent radii of the donor and acceptor must be made. On the basis of X-ray structural results from $Fe(phen)_3^{2+}$ and $Fe(phen)_3^{3+}$ it can be assumed that $a_1 = a_2$ for $[Fe_2(L)_3]^{5+}$.[17] Molecular mechanics calculations can be used to obtain a "van der Waals volume" (VV) for the individual FeL_3 halves of the complexes and a "solvent-excluded" (SE) volume based on van der Waals contact of the solvent. If these two volumes are assumed to be spherical an effective radius for the FeL_3 can be obtained for each. The radius values thus calculated are $a_{VV} = 5.29$ Å and $a_{SE} = 7.41$ Å. Applying eq 4, setting $r = 7.6$ Å gives value of $E_{out} = 3500$ cm^{-1} and 200 cm^{-1}, respectively, for a_{VV} and a_{SE}. Finally, assuming λ_{SO} to be 460 cm^{-1}, values of $E_{OP(VV)} = 4000$ cm^{-1} and $E_{OP(SE)} = 660$ cm^{-1} are obtained from eq 3. Both values are significantly *lower* than the experimental ν_{IT} value listed in Table 3. In order to obtain E_{OP} values of 5000 cm^{-1} from eq 4 a radius $a = 4.86$ Å must be assumed which seems unreasonably small on the basis of X-ray and modeled structures of these complexes. It is entirely reasonable to question the quantitative validity of eq 4 in the present case given that r is considerably less than twice the value of any of the assumed radii. That caveat notwithstanding, it does not appear that the experimental values in Table 3 are exceptionally small. If anything, they are larger than might have been expected.[5,16a]

The present complexes and those for which these continuum dielectric models have been previously applied differ in at least two pertinent ways. First, for cases where the complexes are clearly Robin and Day Class II (i.e., localized valence) the metal−metal separations usually are a good deal larger than the 7.6 Å found in the $[Fe_2(L)_3]^{5+}$ compounds. Second, most of the previously considered systems are linked by a single bridge which excludes less solvent from the region between the donor and acceptor. In contrast, the three bridging linkages

(16) (a) Brunschwig, B. S.; Ehrenson, S.; Sutin, N. *J. Phys. Chem.* **1986**, *90*, 3657. (b) Goodman, B. A.; Raynor, J. B. *Adv. Inorg. Radiochem.* **1970**, *19*, 135.

(17) (a) Baker, J.; Engelhardt, L. M.; Figgis, B. N.; White, A. H. *J. Chem. Soc., Dalton Trans.* **1975**, 530. (b) Zalkin, A.; Templeton, D. H.; Veki, T. *Inorg. Chem.* **1973**, *12*, 1641.

(18) Cruetz, C. *Prog. Inorg. Chem.* **1983**, *30*, 1 and references therein.

(19) Cannon, R. D. *Chem. Phys. Lett.* **1977**, *49*, 299.

(20) Brown, G. M.; Sutin, N. *J. Am. Chem. Soc.* **1979**, *101*, 883.

of $[Fe_2(L)_3]^{5+}$ completely exclude solvent from a solid cone equal to >30% of the total volume around each metal center (estimated from space-filling models). Thus, the $[Fe_2(L)_3]^{5+}$ are effectively "less-solvated" than complexes which are more accessible to solvent in this region, and the effect of this will be to reduce the total magnitude of E_{out}.

A second feature of the ν_{IT} data in Table 3 requiring comment is the larger relative value for $[Fe_2(420)_3]^{5+}$ compared to the other three complexes. Calculated van der Waals volumes (*vide supra*) for the four $[Fe_2(L)_3]$ complexes indicate that $[Fe_2(420)_3]$ is smaller (ostensibly due to the bridges) than the average volume of the other three complexes by ca. 5%. This difference is modest and obviously by itself cannot account for the relative differences in ν_{IT} (Table 3); however, in the absence of more sophisticated dielectric models than are available, it is difficult to assess how much E_{out} would be affected by modest changes in the volume excluded by the bridges. Additionally, careful examination of the energy parameters obtained from the molecular mechanics calculations reveals that there is a significant torsional strain energy (ca. 1000 cm^{-1}) in the bipyridines of $[Fe_2(420)_3]^{5+}$ which is absent in the other compounds. This strain energy might translate into an innersphere component to the reorganizational energy which is absent from the other complexes. Without detailed information on the solvent dependence[21] of ν_{IT}, however, one can only speculate about the origins of the larger value of E_{op} for $[Fe_2(420)_3]^{5+}$. Nonetheless, while the relative difference between ν_{IT} for $[Fe_2(420)_3]^{5+}$ and the other three complexes is large, the absolute difference is relatively small, smaller than the typical margin of error for the various theoretical models that predict E_{in} and E_{out}.

Finally, since the spectral titrations represented by the data in Table 3 were conducted in fairly concentrated solution (ca. 0.02 M) the possibility of ion-paring effects on these data needs consideration. Hendrickson et al. observed significant blue shifts in ν_{IT} (ca. 700 cm^{-1}) for mixed-valence biferrocenes as functions of concentration in low dielectric constant solvents. These shifts were attributed to ion-paring.[22a] In contrast, Hupp et al. examined the concentration dependence of ν_{IT} for $[(NH_3)_5Ru(4,4'\text{-bipy})Ru(NH_3)_5]^{5+}$ in acetonitrile and found no spectral shifts over the concentration range from millimolar to "infinitely dilute".[22b] We have conducted microelectrode voltammetry of I in acetonitrile, in both the presence and absence of added supporting electrolyte (up to 0.1 M $TBAPF_6$), and found no measurable shifts in $E_{1/2}$ for the metal-centered oxidations.[6] These electrochemical results and the spectral results of Hupp et al. lead us to conclude that ion-paring effects are likely not a major concern in acetonitrile at the concentrations employed to generate the data in Table 3; however, minor ion-pairing effects cannot be entirely ruled out.

Theoretical Models for H_{12}. The experimental values of H_{12} in Table 4 may be compared with theoretical values obtained from configuration interaction (CI) calculations carried out for the $[Fe_2(L)_3]^{5+}$ complexes using the INDO/S method developed by Zerner and co-workers.[23] Previous studies[24] have shown that this method yields reliable values of H_{12} for a variety of self-exchange processes involving transition metal complexes. In the present study, instead of evaluating H_{12} directly from charge-localized diabatic states obtained from self-consistent-field (SCF) calculations, as was done in the past,[24c] we adopt the alternative of obtaining the *adiabatic* states within the framework of a 2-configuration CI calculation. The desired *diabatic* quantities (H_{12} and the effective donor/acceptor (D/A) separation distance, r_{DA}) are then evaluated by application of the generalized Mulliken−Hush (GMH)[25] method, using the calculated vertical energy gap between adiabatic states, $E_{op} = h\nu_{IT}$, and the adiabatic dipole moment shift, $\Delta\vec{\mu}$, and transition dipole, $\vec{\mu}_{tr}$

$$H_{12} = \{\mu'_{tr}/((\Delta\vec{\mu})^2 + 4(\mu'_{tr})^2)^{1/2}\}(h\nu_{IT}) \quad (5)$$

$$r_{DA} = ((\Delta\vec{\mu})^2 + 4(\mu'_{tr})^2)^{1/2}/e \quad (6)$$

where μ'_{tr} is the component of $\vec{\mu}_{tr}$ along the $\Delta\vec{\mu}$ direction and e is the magnitude of the electronic charge. Equation 5 may be reexpressed in the familiar Mulliken−Hush (MH)[7,8,26] form by using eq 6:

$$H_{12} = (\mu'_{tr}/er_{DA})(h\nu_{IT}) \quad (7)$$

In conventional applications of the MH model, r_{DA} in eq 7 has been estimated by using the distance separating the *assumed* centroids of donor and acceptor sites.[26b] In the GMH approach,[25] the assumed diagonal form[27] of the two-state dipole moment matrix in the charge-localized diabatic basis leads to the expression for r_{DA} given in eq 6. Although r_{DA} evaluated in this manner may differ appreciably from estimates based on molecular geometry,[25,28,29] we find in the present case (see Table 1) that the Fe−Fe separation is indeed a good estimate.

The two electronic configurations employed in the calculations may be represented as

$$\chi_1^0 = (\text{core})\phi_1 \quad (8a)$$

$$\chi_2^0 = (\text{core})\phi_2 \quad (8b)$$

where (core) is an $(n-1)$-electron core (n is the total number of electrons in the $[Fe_2(L)_3]^{5+}$ complex), which by construction is common to both χ_1^0, and χ_2^0, and where the molecular orbitals (MO) ϕ_1 and ϕ_2 are orthonormal linear combinations of the effective D and A orbitals in the electron transfer process. These latter orbitals are expected to be dominated by the 3d atomic orbitals (AO) of the Fe atoms, but with important tails extending onto the tethered bipyridine ligands. The final eigenfunctions χ_1 and χ_2 (i.e., adiabatic states) are obtained by configurational mixing of χ_1^0 and χ_2^0. The desired quantities H_{12} and r_{DA} are then evaluated from eqs 5 and 6 using the energies and dipole and transition moments in the χ_1, χ_2 basis. The resulting H_{12} may be understood as the coupling element in the charge-localized diabatic basis (ψ_1, ψ_2) obtained by a unitary transformation of χ_1 and χ_2 according to the GMH procedure.[25] Correspondingly er_{DA} is the dipole moment difference in the ψ_1, ψ_2 basis.

(21) For a variety of reasons including the very low value of ν_{IT}, the solubility of the complex, the low value of ϵ_{IT}, and the very positive value of $E_{1/2}(4+/5+)$, solvent studies have not yet been undertaken.

(22) (a) Lowery, M. D.; Hammack, W. S.; Drickamer, H. G.; Hendrickson, D. N. *J. Am. Chem. Soc.* **1987**, *109*, 8019. (b) Hupp, J. T.; Dong, Y.; Blackbourn, R. L.; Lu, H. *J. Am. Chem. Soc.* **1993**, *97*, 3278.

(23) (a) Zerner, M. C.; Loew, G. H.; Kirchner, R. F.; Mueller-Westerhoff, U. T. *J. Am. Chem. Soc.* **1980**, *102*, 589. (b) ZINDO: A comprehensive semiempirical SCF/CI package written by M. C. Zerner and co-workers, University of Florida, Gainesville, FL.

(24) (a) Newton, M. D. *J. Phys. Chem.* **1991**, *95*, 30. (b) Newton, M. D.; Ohta, K.; Zhong, E. *J. Phys. Chem.* **1991**, *95*, 2317. (c) Newton, M. D. *Chem. Rev.* **1991**, *91*, 767.

(25) Cave, R. J.; Newton, M. D. *Chem. Phys. Lett.* **1996**, *249*, 15.

(26) (a) Reimers, J. R.; Hush, N. S. *J. Phys. Chem.* **1991**, *95*, 9773. (b) Creutz, C; Newton, M. D.; Sutin, N. *J. Photochem. Photobiol. A: Chem.* **1994**, *82*, 47.

(27) The validity of this assumption has been demonstrated by more detailed calculations, which take explicit account of the expansion coefficients for the orbital and CI eigenfunctions (Cave, R. J.; Newton, M. D. To be published).

(28) Shin, Y.-G. K., Brunschwig, B. S.; Creutz, C.; Sutin, N. *J. Am. Chem. Soc.* **1995**, *117*, 8668.

(29) Newton, M. D.; Cave, R. J. In *Molecular Electronics*; Jortner, J., Ratner, M. A., Eds.; Blackwell Science Ltd., Oxford, in press.

In order to provide a balanced treatment of the relevant two-state space, the orbitals defining χ_1^0 and χ_2^0 (eq 8) were obtained from a state-averaged SCF calculation based on 50−50 weighting of χ_1^0 and χ_2^0. In each case the ϕ_1, ϕ_2 pairs were dominated (70−100% of the total orbital populations) by $3d_{z^2}$-type AO's at the two Fe sites, where the *z*-axis is defined by the Fe−Fe vector. The remainder of the ϕ_1, ϕ_2 populations involve the orbitals of the bipyridine ligands. As a result of the $3d_{z^2}$ orbital dominance, the relevant dipole moment vectors in the 2−state (χ_1, χ_2) model are all aligned along the Fe−Fe direction (to within ≤0.05D). The $3d_{z^2}$ orbitals belong to the t_{2g} manifolds of the Fe atoms since the *z*-axis as defined here corresponds roughly to a common trigonal axis of the quasi octahedral coordination shells.

The H_{12} values obtained (via eq 5) from the CI results (χ_1, χ_2) are displayed in Table 4. For the three-atom bridge cases (430, 4O0, and 4S0) the calculated and experimental values are in agreement essentially to within experimental uncertainty. The calculated gap between the two-atom and three-atom bridge results is quite small in contrast to the larger gap obtained from experiment.

To provide more perspective on the mechanism of D/A coupling, we also carried out a series of calculations in which the bridges linking the bipyridines were removed and the dangling bonds "tied off" with H atoms, all other atoms in each complex being maintained in their original positions. These results indicate that the three-atom bridges are not important for the overall coupling, which may be understood as direct or "through-space" (TS) coupling between adjacent bipyridine ligands of the respective Fe sites. On the other hand, removing the ($-CH_2CH_2-$) bridges in the 420 complex has a dramatic doubling effect on the H_{12} value, thus suggesting a destructive interference between the TS coupling and the "through-bond" (TB) coupling mediated by the ($-CH_2CH_2-$) bridges. Analogous but less dramatic effects have been found for even-membered trans-staggered alkane bridges,[30] but detailed comparison with the present results is complicated because of the gauche conformation characterizing the bridges in the 420 complex. Since all the bridge-free complexes have similar Fe−Fe separations (by construction, the same as those for the bridged cases listed in Table 1), it might seem surprising that the H_{12} values are not more similar in magnitude. The difference that is in fact observed (97 cm^{-1} *vs* the 48−60 cm^{-1} range for the other cases) points to the important role played by local stereochemistry of the bipyridine pairs between which the TS coupling occurs.

As a test of the above reasoning we have carried out calculations of D/A coupling in radical cations of the type $((CH_2)(-CH_2-)_n(CH_2))^+$, $n = 2$ and 3, with geometries taken from the alkane bridges of the 420 and 430 complexes together with the carbon atoms of the bipyridine moieties at the points of attachment to the bridges. These latter carbon atoms, in the form of terminal CH_2 groups, serve as the D and A sites in these model electron-transfer systems. Radical cations (as opposed to anions) were chosen as being the most relevant analogs for the full complexes, where the low-lying ligand to metal charge transfer (LMCT) states are likely to make "hole" transfer (as opposed to "electron transfer") the more important bridge-mediated process.[24c] Calculations yield comparable values of H_{12} for the $n = 2$ (∼1400 cm^{-1}) and $n = 3$ (∼2100 cm^{-1}) cases. Removal of the bridges as described above, keeping the coordinates of the terminal CH_2 groups fixed, has only a modest effect on H_{12} for $n = 3$ ($H_{12} = 2700$ cm^{-1}), whereas for $n = 2$ the magnitude is greatly enhanced ($H_{12} = 6700$ cm^{-1}). Thus, the behavior of the isolated bridge moieties mimics the H_{12} trends of the full 420 and 430 complexes, supporting the notion that the three-carbon bridges have little role in the coupling, in contrast to the large degree of destructive interference between TS and TB contributions in the case of the two-carbon bridges. We emphasize that the TS coupling invoked here is a local type (between bipyridine carbons in close proximity), as opposed to the negligible long-range TS coupling between the D and A sites (i.e., the Fe atoms).

(30) Liang, C.; Newton, M. D. *J. Phys. Chem.* **1993**, *97*, 3199.

Conclusions

In several important ways, the complexes under consideration here are unique. First, they have very small metal−metal separations yet they remain weakly coupled and, thus, valence-localized. For comparison, dinuclear ruthenium complexes having 4,4′-bipyridine as bridging moieties have significantly larger metal−metal separations (ca. 11.3 Å) and typically exhibit couplings in the 3+/2+ mixed valence form which are 100 cm^{-1} or greater.[18,31] In order to achieve distances comparable with the complexes considered here bridging ligands such as pyrazine have been employed (ca. 6.9 Å).[18,31] With such ligands, however, the metal−metal coupling is greatly enhanced via orbital mixing through the delocalized π-system of the ligand.[31]

The small donor/acceptor separation is consistent with the experimentally observed low value of E_{op}. Furthermore, the lower values of E_{op} for the complexes containing three atoms in the bridge relative to that for $[Fe_2(420)_3]^{5+}$ can be rationalized, at least in part, on the basis of differences in the ability of solvent to access the bridging region and on differences in torsional strain.

The fact that the bridges do not, for the most part, contribute to the donor/acceptor coupling was not anticipated *a priori*. However, in retrospect, given the small separation of the bipyridine ligands it is not altogether surprising. In fact, the center-to-center separation in these systems is considerably shorter than what is generally assumed in the bimolecular 3+/2+ self-exchange reaction for $[M(bpy)_3]$.[5] The fact that the two-methylene bridge appears to interfere with the direct coupling mediated by the bipyridine rings was surprising. We have at our disposal other bridged bipyridine ligands which should allow the preparation of analogous complexes in which the metal−metal separation can be systematically increased, albeit without maintaining the same relative bipyridine orientations as was possible here. Nonetheless, at some D/A separation the bridge-mediated coupling should begin to dominate the direct coupling. Once this occurs a distance dependence typical of through-σ-bond coupling should be observed.[30] However, such studies will almost certainly require a different experimental approach given that the present complexes already exhibit IT transitions which are so weak as to be on the edge of accurate experimental measurability.

Finally, the excellent agreement between the experimentally and theoretically determined H_{12} values is noteworthy, especially considering the relative complexity of these systems from a theoretical standpoint. The agreement supports the validity of the compact picture of the coupling which emerges from the theoretical results, one dominated by a pair of t_{2g} 3d orbitals on the respective Fe atoms (the "axial" $3d_{z^2}$ orbitals), whose interaction is mediated via superexchange by the π-type MO's of the bipyridine ligands. Analysis of the theoretical results in

(31) (a) Creutz, C.; Taube, H. *J. Am. Chem. Soc.* **1969**, *91*, 3988. (b) Creutz, C.; Taube, H. *J. Am. Chem. Soc.* **1973**, *95*, 1086. (c) Callahan, R. W.; Brown, G. M.; Meyer, T. J. *Inorg. Chem.* **1975**, *14*, 1443. (d) Goldsby, K. A.; Meyer, T. J. *Inorg. Chem.* **1984**, *23*, 3002.

terms of the recently developed Generalized Mulliken Hush model not only yields H_{12} values but also values of effective donor/acceptor separation, independent of any assumptions based on molecular structure. The values so obtained in the present case turn out to equal r_{M-M} to within 0.01 Å.

Acknowledgment. The authors acknowledge support of this work from the Division of Chemical Sciences, Office of Basic Energy Science, U.S. Department of Energy, under grants DE-FG02-92ER14301 (C.M.E.) at Colorado State University and DE-AC02-76CH00016 (M.D.N.) at Brookhaven National Laboratory. The authors also wish to thank Professor A. K. Rappé and Dr. Carol Creutz for helpful discussions.

Supporting Information Available: Descriptions of materials and instrumentation and experimental details for compounds **I**−**IV** (3 pages). Ordering information is given on any current masthead page.

JA954297Q